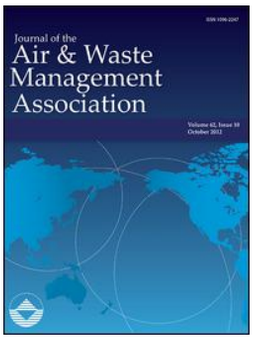

Taylor & Francis
Taylor & Francis Group

Journal of the Air & Waste Management Association

ISSN: 1096-2247 (Print) 2162-2906 (Online) Journal homepage: informahealthcare.com/journals/uawm20

Design and Characterization of a Two-Stage Human Subject Exposure Chamber

Roman Y. Kuprov, David Buck, C. Arden Pope III, Delbert J. Eatough & Jaron C. Hansen

To cite this article: Roman Y. Kuprov, David Buck, C. Arden Pope III, Delbert J. Eatough & Jaron C. Hansen (2011) Design and Characterization of a Two-Stage Human Subject Exposure Chamber, Journal of the Air & Waste Management Association, 61:8, 864-871, DOI: 10.3155/1047-3289.61.8.864

To link to this article: https://doi.org/10.3155/1047-3289.61.8.864

Published online: 10 Oct 2011.

TECHNICAL PAPER

ISSN:1047-3289 *J. Air & Waste Manage. Assoc.* **61**:864–871
DOI:10.3155/1047-3289.61.8.864

Design and Characterization of a Two-Stage Human Subject Exposure Chamber

Roman Y. Kuprov and David Buck
Department of Chemistry and Biochemistry, Brigham Young University, Provo, UT

C. Arden Pope III
Department of Economics, Brigham Young University, Provo, UT

Delbert J. Eatough and Jaron C. Hansen
Department of Chemistry and Biochemistry, Brigham Young University, Provo, UT

ABSTRACT

A human subject exposure chamber, designed to hold six to eight subjects, coupled to an approximately 30-m^3 Teflon reaction bag was designed and built to provide exposures that mimic the production and photochemical oxidation of atmospheric pollutants resulting from the combustion of coal or wood from a stove. The combustion products are introduced into the Teflon bag under atmospheric conditions. Photochemical oxidation of this mixture is accomplished by exposure to tropospheric sunlike radiation from an array of ultraviolet and black lamps. The aerosol in the Teflon reaction bag is then transferred into the exposure room to maintain a constant, lower exposure level. Continuous and semicontinuous monitoring of the gas and particulate matter (PM) pollution in the exposure room and the reaction bag is accomplished using a suite of instruments. This suite of instruments allows for the measurement of the concentrations of total and nonvolatile PM, nitric oxide, nitrogen dioxide, carbon monoxide, carbon dioxide, and ozone. The concentration of the particles was monitored by an R&P tapered element oscillating microbalance monitor. The chemical composition of the PM and its morphological characterization is accomplished by collecting samples in filter packs and conducting ion chromatography, elemental X-ray fluorescence, and scanning electron microscopy analyses. The concentration and composition of emissions from combustion of wood and coal is described. The results of this study suggest that although the bulk compositions of particulate emissions from the combustion of coal or wood in a stove have many similarities, the wood smoke aerosol is photochemically reactive, whereas the coal smoke aerosol is not.

IMPLICATIONS

The presence of high concentrations of PM and ozone in air has been linked to exacerbation of cardiovascular and cerebrovascular health problems. This manuscript describes the design of a human subject exposure chamber that allows for the production and control of PM and atmospherically important gases and characterizes pollutants present in the exposure chamber from the combustion of wood and coal. Fresh and photochemically aged pollutants are characterized. The chamber thus allows for studies to be conducted to quantify the effects of short-term PM and gas exposure on human subjects.

INTRODUCTION

The most frequent cause of death among adults in the United States is disease of the heart (principally heart attacks), followed by cancer and cerebrovascular diseases (stroke).[1] Two of the three main causes are related to the function of the cardiovascular system. Long-term exposure to elevated levels of particulate matter (PM) pollution have been implicated in the increased risk of the onset of ischemic heart disease and subclinical chronic inflammatory lung injury and atherosclerosis.[2] A proposed mechanism for the effects of PM exposure on the cardiovascular system is via an inflammatory response of the endothelium.[3] The exposure of heritable hyperlipidemic rabbits and mice to elevated, environmentally relevant PM concentrations has been shown to accelerate the progression of atherosclerotic plaques and vascular inflammation.[4,5] Short-term exposure to elevated and acute levels of PM was found to cause an increase in fibrogen and inflammatory markers in the pulmonary and respiratory systems of humans.[6–8]

The connection of short-term PM exposure and the onset of myocardial infarction has been observed in general population studies.[9–11] Additionally, a crossover study of 12,865 patients living in Utah showed that short-term exposure to high PM levels contributed to acute coronary disease, especially among the individuals predisposed to or with a current coronary condition.[12,13] Acute vasoconstriction was observed in healthy adults after short-term exposure to levels of fine particulate pollution and ozone common in urban areas.[14] Recent work has also shown the effects of wood smoke on human health.[15,16] Although the effects of exposure to ambient pollution in humans has been studied, and the effects of exposure of experimental animals to concentrated ambient particulate material has been reported in several studies, a study of the endothelial function effects of direct,

short-term exposure of humans to PM in laboratory conditions has not yet been performed.[17–19]

Several designs for controlled human exposure have been developed. These include full-body exposure chambers,[20,21] hoods,[22] and masks.[23] PM generation in these systems uses on-board production of pollution via previously obtained powder samples (wheat flour, dust, etc.) or the use of the particulate pollution directly extracted and concentrated from ambient atmospheric conditions. Exposure facilities that allow for direct exposure of human subjects to diesel exhaust generated using controlled dynamometer procedures[24] or to real-world mobile exhaust in a van modified to serve as an exposure facility on Los Angeles freeways[25] have been recently described.

This paper describes the design and characterizes the performance of a two-stage exposure chamber for human subjects developed to study the effects of short-term PM exposure. The design of this chamber allows for the measurement of (1) the concentrations of generated PM using semicontinuous monitors; (2) the composition of the PM in integrated samples; and (3) the concentrations of environmentally relevant gases, including carbon monoxide (CO), carbon dioxide (CO_2), oxides of nitrogen (NO_x), and ozone (O_3). Additionally, the current design allows for the pretreatment of the aerosol before introduction of the aerosol to the human exposure chamber. Studies with untreated aerosol and in which the aerosol was photochemically aged via exposure to ultraviolet (UV) radiation to further simulate actual daytime tropospheric conditions were conducted.

EXPERIMENTAL DESIGN

Exposure Facility Design

Figure 1 shows a schematic of the exposure room and PM/gas conditioning system. The exposure facility is comprised of two separate compartments: an approximately 363-m^3 Teflon bag (elliptical in shape and collapsible as air is removed from the bag, with maximum dimensions of 8.2 × 4.6 × 2.3 m and the approximately 27-m^3 exposure room (3.6 × 2.9 × 2.6 m high). The structure is two stories with the bag location above the exposure room and monitoring equipment. The smaller area on the second floor has a wall along the bag length to protect personnel working the larger first floor of the facility below the bag from UV radiation. The Teflon bag is designed to contain the source PM during an experiment and photochemical pretreatment of the PM is done in the bag. The Teflon bag and associated sampling equipment and UV lamps have been previously described.[26]

The bag is constructed of 0.3-mm thick Teflon film that is heat-sealed with a Vertrod sealing blade iron. A 3-in. wide (7.5 cm) adhesive polysilicone tape (R.S. Hughes Co., Inc., no. 8403) was laid over each seam to provide additional structural integrity and shape to the bag. Teflon film was used because of Teflon's chemical inertness and high transmission of UV radiation, which is used to photochemically age the PM inside of the bag.

A utility manifold at the bottom of the Teflon bag allows for instrumentation interface as well as air and combustion emissions delivery. Sampling tubes that enter the bag via a Teflon manifold are stainless steel or Teflon to decrease reactivity with the contents.

Additionally, an in-bag fan with Teflon-coated blades extends through the manifold to gently stir the contents of the bag. Acceptable mixing of the PM inside of the bag was achieved at 40–50 rpm. Higher rotation speeds resulted in increased particle deposition to the walls of the bag.

To simulate photochemical atmospheric conditions, a set of 200 F40BL GE black lights (maximum output at 365 nm, irradiance of 0.28 W/m^2/nm) and 12 FS40UVB (maximum output at 312 nm, irradiance of 0.38 W/m^2/nm) lamps from Commercial Lighting (SLC) were placed above the Teflon bag. To ensure homogeneous light distribution, the lamps were set 30 cm apart and distributed across the ceiling above the bag. The details on UV and black lamp outputs are available from the manufacturer.

Accommodations for subjects within the exposure room included a small sofa, four chairs, a small desk, and a small refrigerator. During the exposure experiments the room contained up to six subjects.[27] The room was isolated from the building's ventilation system to avoid unnecessary loss and dilution of PM. To avoid loss of PM when subjects

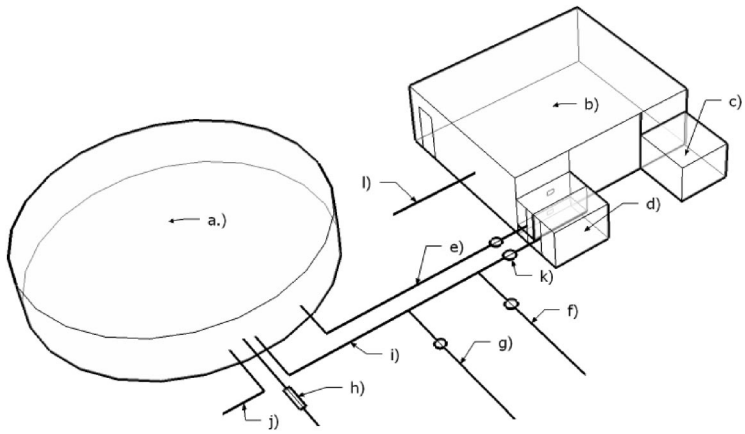

Figure 1. Diagram of the human exposure chamber: (a) Teflon bag; (b) human exposure chamber; (c) internal air circulation pump; (d) bag-chamber transfer pump; (e) bag-to-chamber transfer line; (f) bag purge line; (g) clean air filling line; (h) combustion emissions intake line and catalyst; (i) chamber-to-bag transfer line; (j) bag sampling manifold, UV lights not shown; (k) particle control transfer values; and (l) chamber sampling manifold. The sampling manifolds are also used in conjunction with item e.

entered and exited the room, two layers of heavy Teflon film were fastened to the door frame to create a veil with overlapping flaps. This significantly reduced the amount of PM dissipated into the areas outside of the exposure room when opening and closing the door. With the door open, gases may disperse between the flaps of the Teflon strips into the outside area, but most PM is retained. This provided a mechanism whereby concentrations of nitric oxide (NO), nitrogen dioxide (NO_2), CO, CO_2, and O_3 could be lowered while maintaining the PM concentration in the exposure room. During exposure experiments, the gas and particle concentrations in the exposure room were continuously measured simultaneously.

An internal circulation blower with a pumping capacity of approximately 1 m^3/min was attached to the exposure room to provide circulation and a homogeneous mixture of PM in the exposure room. To ensure a homogeneous mixture, the internal circulation vents were placed opposite of each other near the floor and the ceiling of the room. The blower was operated at all times during the human exposure experiments. Although the constant motion of air through the air circulation system increased the PM loss to the walls of the room, this disadvantage was necessary to maintain a homogeneous PM mixture in the exposure room.

Particle Concentration Control and Transfer

Wood and coal were used as fuels for the generation of PM. The generation of PM concentrations between 175 and 200 $\mu g/m^3$ from the combustion of coal or photochemically aged wood for several hours was evaluated. Coal and wood were used as fuels for particle generation in part because of their universal use and because the chemical composition of PM generated during their combustion was expected to be different. Before the start of an exposure experiment, the bag was filled with dry, filtered laboratory air. The PM was generated by burning coal or wood in a Regency wood burning stove (see Figure 2). Between 6 and 12 experiments were performed on coal and photochemically aged wood smoke. Coal was obtained from the Brigham Young University heating plant. The nominal ash and sulfur content was 9.35 and 0.48%, respectively. Dried pine wood was purchased from a local grocery store (Hotwood, California Hotwood, Inc.). All wood used came from the same lot. A fraction of the emissions were directed from the smoke stack into the Teflon bag after at least 15 min of a steady rate of burning.. The aerosol was transferred into the Teflon bag through a 2.5-cm diameter steel tube attached to the stove smoke stack using a squirrel cage blower. Before entering the bag, the emissions were passed over a ceramic honeycomb, magnesium-oxide-supported gold catalyst heated to 85–90 °C. The catalyst converts CO into CO_2 with approximately 95% efficiency with minimal loss of PM. Total or even partial oxidation of gas-phase organic compounds likely to be present in the aerosol by the gold catalyst under these conditions is unlikely because significantly higher temperatures are required for activation of C–C and C–H bonds by molecular oxygen on this particular catalyst, although gold supported on carbon in a certain crystallite size range is apparently active for epoxidation of specific alkenes in the same temperature range as in the study presented here.[28]

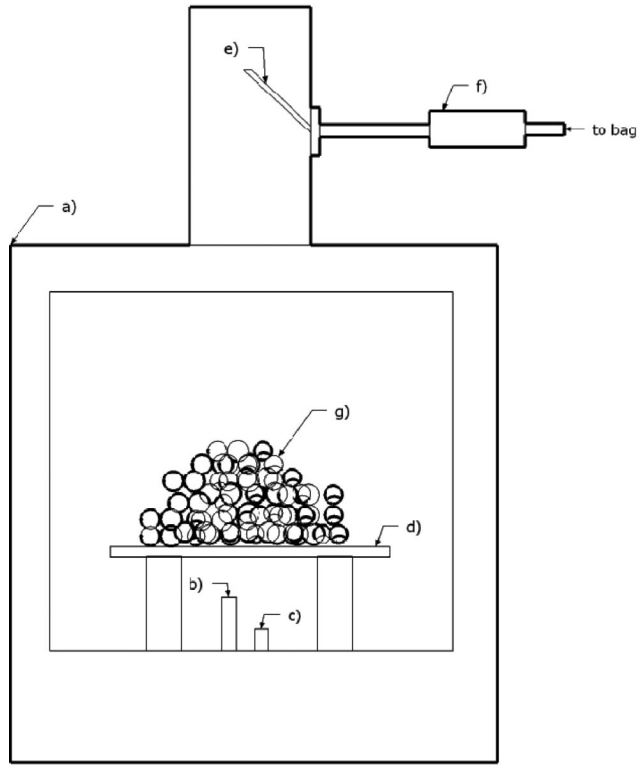

Figure 2. Oven setup for burning wood or coal: (a) oven, (b) Bunsen burner (used only for coal ignition), (c) air supply tube, (d) stainless steel mesh, (e) PM intake tube, (f) catalyst enclosure, and (g) fuel (coal or wood).

When burning wood, a slightly opened oven door provided sufficient airflow to maintain a steady combustion rate. In the case of coal, additional airflow was provided into the stove via a tube connected to a pressurized laboratory air source inserted through the bottom air intake of the stove to facilitate a more complete and steady combustion. Coal combustion temperatures were estimated visually from the color of the flame.[29] Relatively high combustion temperatures (>600 °C for wood and >1000 °C for coal) were required for production of smaller size PM and a more complete decomposition of long-chain hydrocarbons. Lower combustion temperatures (<500 °C and <800 °C for wood and coal, respectively) resulted in quick failure of the tapered element oscillating microbalance (TEOM) and filter dynamics measurement system (FDMS)-TEOM because of rapid deposition of char on the microbalance filters that prohibited airflow through the instrument. This was avoided at higher burn temperatures. If photochemically aged PM was to be generated, the UV-black lights were turned on at the time of infusion of the wood smoke into the bag and remained on for the duration of the experiment. Introduction of photochemically aged aerosol into the room occurred after the initial hour of aging.

The room and the Teflon bag were connected via two 2-in. (~5-cm) diameter polyvinyl chloride transfer pipes with a valve system through which the delivery of PM into the exposure room could be controlled (see Figure 1).

The pipes were connected directly into the bag through the Teflon manifold. Transfer of PM from the bag into the room was done through a high-volume transfer blower attached to the side of the exposure room. The blower transfers the room air into the bag through one of the transfer pipes, creating a pressure differential between the bag and the room. The second transfer pipe is opened to allow for transfer of the Teflon bag contents into the exposure room. A small fan was installed in the ventilation orifice on the exposure room side to aid in the transfer of the PM from the bag.

FDMS-TEOM (R&P Model 8400) and TEOM (R&P Model 1400a) monitors were attached to the bag manifold to monitor the concentration of total and nonvolatile PM, respectively. To keep the PM concentration inside of the exposure room within the desired value (175–200 $\mu g/m^3$), the PM concentration inside of the bag needed to be approximately 1200 $\mu g/m^3$. Concentrations higher than 1800 $\mu g/m^3$ inside of the Teflon bag caused rapid microbalance filter overload in the FDMS-TEOM and TEOM. Running 10-min averages of the PM concentration in the room were recorded every 10 sec by the TEOM instrument (filter temperature was set to 30 °C, main flow 3.00 standard L/min, auxiliary flow 13.64 standard L/min). A running 15-min average of semi-volatile and nonvolatile PM in the bag and room was recorded with FDMS-TEOM every 15 min (filter temperature at 30 °C, main flow 3.00 standard L/min, auxiliary flow 13.64 standard L/min).

The conditions in the exposure room were monitored through a stainless steel manifold internally coated with Teflon. The manifold was attached to a 1-in. diameter stainless steel pipe (~2 m in length) that was inserted into the exposure room. The manifold allowed for attachment of another set of TEOM and FDMS-TEOM instruments; CO (Thermo, Inc., model 42), NO, NO_x (Thermo, Inc., model 48), and O_3 (Dasibi Environmental Corporation, model 1003-PC) concentration meters; and a set of three filter packs (a 47-mm, 0.2-μm Teflon filter [Whatman], a 0.4-μm Nucleopore filter [Whatman], and a 47-mm prefired quartz filter [Gelman Sciences] followed by a 47-mm carbon impregnated glass filter [Schlacer & Schell]). The concentration of CO_2 was monitored via a handheld monitor (Telarie 7001) located in the exposure room. If gas concentrations within the exposure room rose sharply or began to exceed the predetermined experimental values, the door into the exposure room was opened to lower the gas concentrations with little to no particle loss. This method provided an efficient and quick way of controlling the gas concentrations within the room. The rate ($t_{1/2}$ ~15 min) of PM decay inside of the exposure room demanded periodic infusion of PM and gases from the Teflon bag into the room approximately every 10 min. The concentration of PM in the exposure room was controlled by the time interval between and the duration of the infusion events.

RESULTS AND DISCUSSION

Particle Deposition and Coagulation

The half-life of PM in the Teflon bag was determined by a one-time infusion of wood or coal smoke followed by monitoring of the decay rate. Figure 3 displays normalized decay curves for non-aged wood smoke and photochemically aged wood and coal smoke. The decay of non-UV aged coal smoke was indistinguishable from the decay of photochemically aged coal smoke shown in Figure 3 and for this reason is not included in this figure. Production of secondary aerosols because of the reactions attributed to photochemical aging for wood smoke was evidenced by the change in the decay order of the PM as well as the increase in the total particulate concentration. The decay rate of nonphotochemically aged coal and wood smoke was determined to be first order ($k_{wood} = 0.071 \pm 0.00005$ hr^{-1}, $k_{coal} = 0.083 \pm 0.00007$ hr^{-1}; where the uncertainty is reported as 2σ in the fit to the data); however, secondary particle formation during UV exposure of wood smoke shifted the decay rate to be neither first nor second order. The differences in the first-order decay rate for the nonphotochemically aged wood and coal smoke suggest that the processes occurring in the two fresh emissions are different. This can be attributed to enhanced coagulation or deposition losses of coal smoke compared with wood smoke during aging because of differences in particle size distribution or to nonphotochemistry production of wood smoke particles because of gas-phase reactions and/or condensation of semi-volatile material. Which mechanism(s) predominated cannot be deduced from the data obtained. Normalizing the PM concentrations during the decay studies and integrating with respect to time confirmed the production of secondary PM from the wood smoke during UV exposure (see Figure 3). The initial curvature of the photochemically aged wood smoke decay in relation to the other graphs suggests secondary particle formation. Actual PM decay in the bag during the exposure experiments increased because of frequent addition of fresh emissions and mixing with the less concentrated PM mixture from the exposure room.

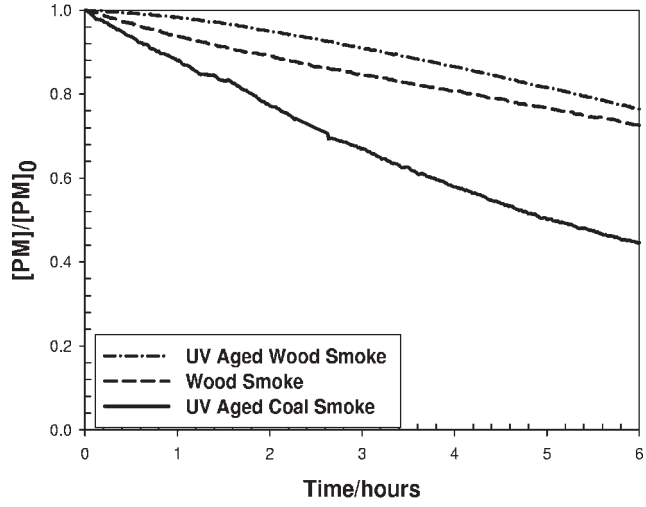

Figure 3. Normalized decay of wood smoke and photochemically aged wood and coal smoke as measured with a TEOM in the Teflon bag. The decay curve for non-aged coal smoke was indistinguishable from that of aged coal smoke and for that reason is not included in this figure. The apparent curvature and elevation of the photochemically aged wood smoke over the regular wood and coal smoke decay plots suggest secondary particle formation. The decay rates display particle decay in the unperturbed bag environment and do not represent the decays observed during the actual experiments.

PM in the exposure room was found to have a significantly faster decay rate than in the Teflon bag. This is due to the constant internal air circulation and the large, noninert surface area of the objects in the room. Subjects entering and leaving the exposure room had little effect on the PM decay rate. However, the PM loss within the exposure room increased with the number of subjects present. Each 6-hr exposure experiment involving human subjects[27] required approximately eight additional combustion emissions infusions into the Teflon bag to keep the concentration above 1200 $\mu g/m^3$ when using coal. Because of the decreased decay rate and secondary particle formation, two additions were needed for photochemically aged wood smoke.

As expected, at high combustion temperatures most of the PM produced was under 2.5 μm, as suggested by scanning electron microscopy (SEM) images of the PM collected on a Nucleopore filter. Figure 4 shows SEM images of PM from coal and photochemically aged wood smoke collected directly from the Teflon bag. Particles from coal and photochemically aged wood smoke collected on Nucleopore filters were centered around 50–100 nm in diameter. Although particles on the filter tended to cluster, the authors suggest that this clustering was not present in the Teflon bag aerosol but rather is an artifact of sampling. PM from coal had a poorly defined, amorphous shape in contrast to the clusters of spherical particles present in the photochemically aged wood smoke.

Secondary particle formation during photochemical aging of wood smoke was manifest by a decreased rate of loss of PM when compared with unaged PM from wood. In the course of 4 hr, the decline in concentration for coal was nearly 40% of the original value, 20% for wood, and only 10% for photochemically aged wood smoke. Secondary formation of PM due to the reaction of photochemically created organic radicals and unburned hydrocarbons

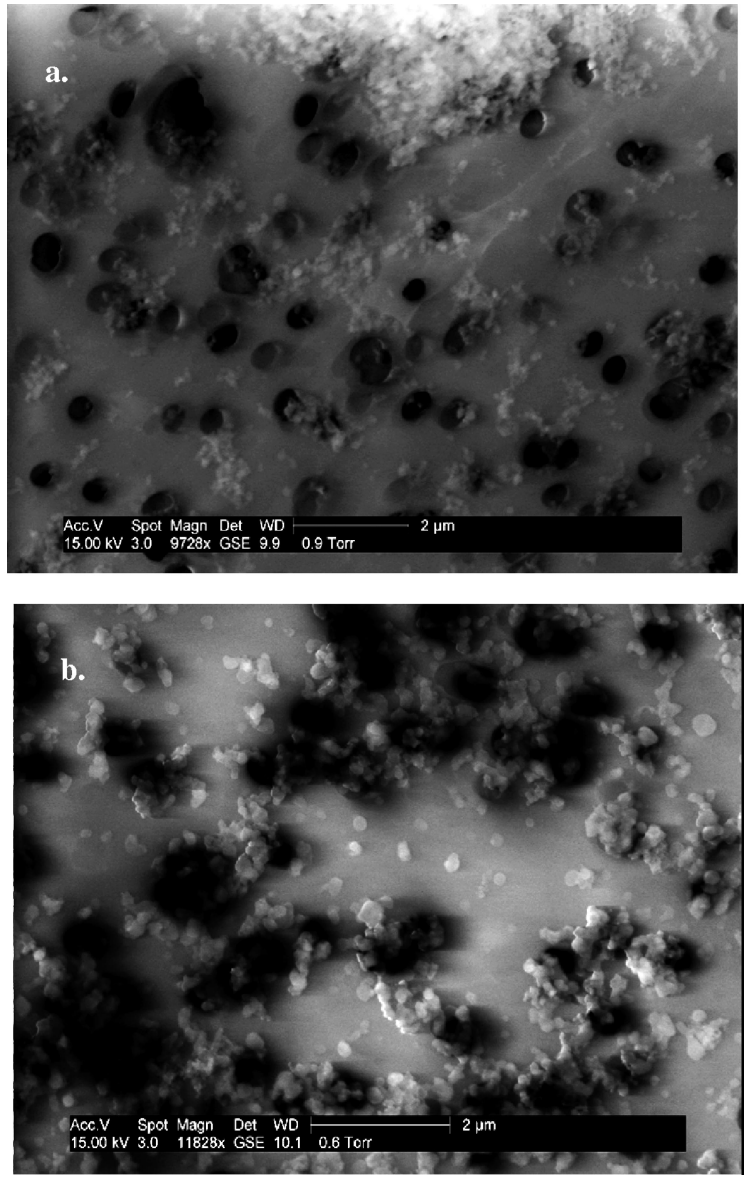

Figure 4. (a) SEM image of coal smoke particles collected on a Nucleopore membrane filter (pore size 0.4 μm). (b) SEM image of photochemically aged wood smoke particles collected on a Nucleopore membrane filter. Both sets of particles are $<$2.5 μm in size but have different textures.

in wood smoke is a plausible explanation for the slower decay of the PM concentration of wood smoke in the bag.

Particle Composition

Chemical characterization of PM was limited to coal and photochemically aged wood smoke particles. Wood smoke and photochemically aged coal smoke were not characterized because neither of these sources was used in human subject exposure experiments. Coal and photochemically aged wood smoke were analyzed for anions with ion chromatography (IC). An IC3000 was used with an IonPac AS14A-5 μm, 3 × 150 mm analytical column produced by Dionex. The eluent was 8 parts per million (ppm) sodium carbonate ($NaCO_3$) and 1 ppm sodium bicarbonate ($NaHCO_3$) aqueous solution. Calibration of the chromatograph was done with the Seven Anion Standard solution provided by Dionex. For IC analyses each filter sample was extracted with 5 mL of deionized water by sonication for at least 15 min. The extracted samples were analyzed three times with a new background reading taken between the samples. The results are shown in Table 1. Coal particles had higher fractions present as chloride and phosphate as well as a slightly higher abundance of sulfate. Wood smoke contained increased amounts of nitrate.

X-ray fluorescence (XRF) analysis was performed with a PANalytical Epsilon 5 XRF analyzer with a Gadolinium (Ga) anode as a source of X-rays and a solid state germanium X-ray detector. Instrument calibration and sample analysis was performed by Desert Research Institute (DRI). Table 2 shows the mass percent of the elements. As expected, sulfur was more abundant in coal smoke PM. Consistent with potassium being a biomass marker, potassium was the most prevalent element in the photochemically aged wood smoke PM.[30,31] The coal smoke PM also had a larger concentration of lead (Pb) relative to the photochemically aged wood smoke PM. Surprisingly, the mercury content of the photochemically aged wood smoke and coal smoke PM was below the detection limit of the instrument (0.001 μg/filter). Chloride content of coal ash found by XRF analysis was identical to that found via IC. A small concentration of iron was also observed in coal ash, most likely originating from pyrites, commonly present in coals. Only 28% of sulfur was detected as sulfate in coal and wood PM. Low sulfate yields may be attributed to formation of organic sulfur compounds as the result of incomplete combustion. Ultrafine coal ash PM (<0.5 μm diameter) is known to contain a measurable amount of thiophenic compounds that are stable at temperatures over 900 °C in air.[6,32–34] Inorganic sulfides are also found as a byproduct of an incomplete combustion of coal even at temperatures as high as 1370 °C in excess oxygen. Additionally, sulfites may have been produced, which would further contribute to the reconciliation of sulfur balance.[33,34] Only sulfate was quantified and the presence of other forms of sulfur must be done by inference.

Total carbon (TC) analysis was performed with a Sunset Laboratories dual-oven TC analyzer.[35] Organic carbon (OC) was converted to OM using a factor of 1.4.[36] The contribution of elemental carbon (EC) and OC to total PM is given in Table 1. Both PM types had nearly identical contents of EC and OM. Figure 5 shows OC, EC, and the EC/TC ratio as a function of time from the infusion of coal smoke into the Teflon bag with the UV lights on. Because of overload of the filters on the instrument, data collected earlier than 270 min are invalid and data are only shown 270 min after infusion of PM into the bag. Within the uncertainty of the data, the EC/TC ratio is constant, consistent with previous observations showing minimal secondary particle formation from coal smoke.

Table 1. Results of ion chromatographic anion analysis of aged wood and coal combustion particles collected from the Teflon bag with 0.4 μm PTFE filters.

	Aged Wood Smoke	Coal Smoke
Cl^-	0.00 ± 0.01%	0.42 ± 0.01%
NO_2^-	0.03 ± 0.00%	0.24 ± 0.01%
NO_3^-	7.01 ± 0.9%	0.52 ± 0.01%
PO_4^{3-}	0.00 ± 0.01%	0.92 ± 0.4%
SO_4^{2-}	1.16 ± 0.01%	1.70 ± 0.01%
EC	23 ± 12%	31 ± 12%
OM	68 ± 12%	58 ± 12%

Notes: Concentrations are given as the mass percentage of the total weight of the collected PM. Uncertainty is given as absolute error in the percentage. Two filter samples were analyzed.

Table 2. X-Ray fluorescence elemental analysis data for aged wood and coal combustion particles.

	Aged Wood Smoke	Coal Smoke
K	8.39 ± 0.04%	0.24 ± 0.03%
S	1.36 ± 0.11%	2.01 ± 0.15%
Cl	0.27 ± 0.03%	0.42 ± 0.04%
Zn	0.34 ± 0.02%	0.35 ± 0.02%
Fe	0.00 ± 0.04%	0.14 ± 0.06%
Ca	0.25 ± 0.03%	0.00 ± 0.04%
Pb	0.00 ± 0.04%	0.06 ± 0.06%
Hg	0.00 ± 0.013%	0.00 ± 0.015%

Notes: Concentration of elements expressed in wt/wt % ratio. Two sample filters were analyzed.

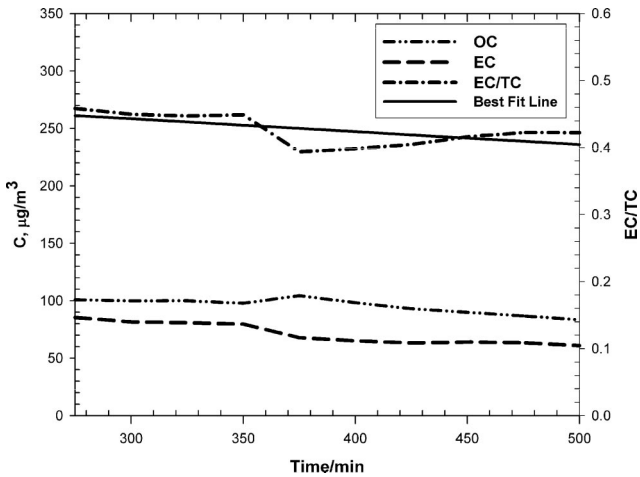

Figure 5. EC, OC, and EC/TC from coal smoke as a function of time with UV photochemical aging.

Stability of Conditions during an Exposure Experiment

Figure 6 shows the conditions (gas and PM) in the exposure room during a typical exposure experiment for non-UV aged wood smoke.[27] Additional details about and PM and gas components during all experiments are given in the companion paper.[27] The presence of subjects inside of the exposure room increased the PM loss rate. To maintain nearly constant exposure conditions during a study with human subjects, aerosol was delivered into the exposure room at 15- to 20-min intervals. Such oscillations in aerosol delivery resulted in the sinusoidal-like graph. In the representative conditions shown in Figure 6, the average concentration throughout the experiment was 190.7 ± 20.5 $\mu g/m^3$ (standard deviation), close to the goal of 175 $\mu g/m^3$.

Peaks in the concentrations of O_3, NO_2, and CO in the exposure room are also correlated with the infusion of fresh aerosol from the bag. CO concentrations averaged 7 ± 1 ppm throughout the duration of a typical exposure experiment. The NO_2 concentration deviated more strongly over the course of an experiment and averaged 35 ± 8 parts per billion (ppb). Average NO concentrations were 4.1 ± 8 ppb. The average O_3 concentration was 54 ± 3 ppb.

CONCLUSIONS

A chamber for human subject exposure experiments was designed and constructed. The design allows for the photochemical pretreatment of PM as well as for real-time control and monitoring of the conditions inside of the bag and the exposure room. PM used in the experiments was chemically and morphologically characterized. The design of the two-stage human exposure chamber presented here offers several distinct advantages. First, the generation and optional pretreatment of the PM happen in a volume separated from the actual human exposure chamber. This allows for close monitoring and control of the PM and gas concentrations before the exposure. Second, the large panel of UV and black lamps directly above the first stage of the chamber provides the option of photochemically aging the PM so as to mimic actual daytime conditions.. Third, the construction of the exposure chamber allows interfacing with a wide range of monitoring and analyzing instruments as well as the collection of PM for chemical and elemental analysis.

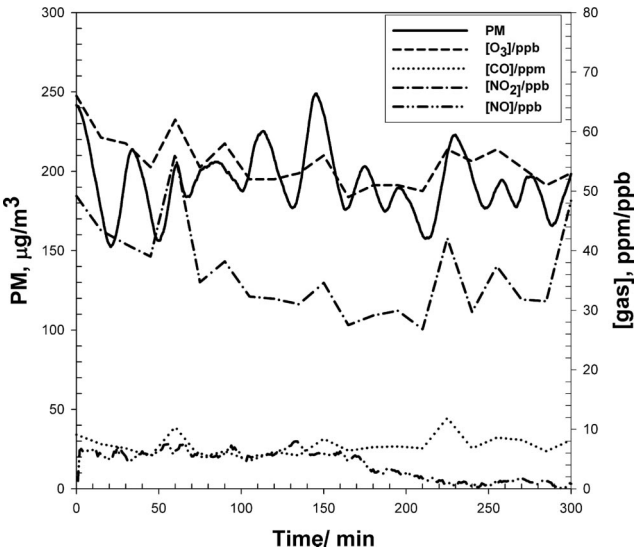

Figure 6. Gas and PM concentrations using photochemically aged wood smoke during a typical human exposure experiment. The average values of concentrations of gases and PM were held under regulatory standards and within experimental protocols.

ACKNOWLEDGMENTS

The authors thank DRI for the XRF analysis. The Microscopy Laboratory at Brigham Young University graciously provided SEM images.

REFERENCES

1. Minino, A.M.; Heron, M.P.; Murphy, S.L.; Kochankek, K.D. Deaths: Final Data for 2004; *Natl. Vital Stat. Rep.* **2007**, *55*, 1-119.
2. Pope, C.A.; Burnett, R.T.; Thurston, G.D.; Thun, M.J.; Calle, E.E.; Krewski, D.; Godleski, J.J. Cardiovascular Mortality and Long-Term Exposure to Particulate Air Pollution—Epidemiological Evidence of General Pathophysiological Pathways of Disease; *Circulation* **2004**, *109*, 71-77.
3. Souza, M.B.; Saldiva, P.H.N.; Pope, C.A.; Capelozzi, V.L. Respiratory Changes Due to Long-Term Exposure to Urban Levels of Air Pollution—a Histopathologic Study in Humans; *Chest* **1998**, *113*, 1312-1318.
4. Suwa, T.; Hogg, J.C.; Quinlan, K.B.; Ohgami, A.; Vincent, R.; van Eeden, S.F. Particulate Air Pollution Induces Progression of Atherosclerosis; *J. Am. Coll. Cardiol.* **2002**, *39*, 935-942.
5. Chow, J.C.; Watson, J.G.; Mauderly, J.L.; Costa, D.L.; Wyzga, R.E.; Vedal, S.; Hidy, G.M.; Altshuler, S.L.; Marrack, D.; Heuss, J.M.; Wolff, G.T.; Pope, C.A.; Dockery, D.W. Health Effects of Fine Particulate Air Pollution: Lines that Connect; *J. Air & Waste Manage. Assoc.* **2006**, *56*, 1368-1380.
6. Sorensen, M.; Daneshvar, B.; Hansen, M.; Dragsted, L.O.; Hertel, O.; Knudsen, L.; Loft, S. Personal $PM_{2.5}$ Exposure and Markers of Oxidative Stress in Blood; *Environ. Health Perspect.* **2003**, *111*, 161-165.
7. Adamkiewicz, G.; Ebelt, S.; Syring, M.; Slater, J.; Speizer, F.E.; Schwartz, J.; Suh, H.; Gold, D.R. Association between Air Pollution Exposure and Exhaled Nitric Oxide in an Elderly Population; *Thorax* **2004**, *59*, 204-209.
8. Ghio, A.J.; Kim, C.; Devlin, R.B. Concentrated Ambient Air Particles Induce Mild Pulmonary Inflammation in Healthy Human Volunteers; *Am. J. Resp. Crit. Care Med.* **2000**, *162*, 981-988.
9. Kunzli, N.; Jerrett, M.; Mack, W. J.; Beckerman, B.; LaBree, L.; Gilliland, F.; Thomas, D.; Peters, J.; Hodis, H.N. Ambient Air Pollution and Atherosclerosis in Los Angeles; *Environ. Health Perspect.* **2005**, *113*, 201-206.
10. Peters, A.; Dockery, D.W.; Muller, J.E.; Mittleman, M.A. Increased Particulate Air Pollution and the Triggering of Myocardial Infarction; *Circulation* **2001**, *103*, 2810-2815.
11. Zanobetti, A.; Schwartz, J. The Effect of Particulate Air Pollution on Emergency Admissions for Myocardial Infarction: a Multicity Case-Crossover Analysis; *Environ. Health Perspect.* **2005**, *113*, 978-982.
12. Sullivan, J.; Sheppard, L.; Schreuder, A.; Ishikawa, N.; Siscovick, D.; Kaufman, J. Relation between Short-Term Fine-Particulate Matter Exposure and Onset of Myocardial Infarction; *Epidemiology* **2005**, *16*, 41-48.
13. Pope, C.A.; Muhlestein, J.B.; May, H.T.; Renlund, D.G.; Anderson, J.L.; Horne, B.D. Ischemic Heart Disease Events Triggered by Short-Term Exposure to Fine Particulate Air Pollution; *Circulation* **2006**, *114*, 2443-2448.
14. Brook, R.D.; Brook, J.R.; Urch, B.; Vincent, R.; Rajagopalan, S.; Silverman, F. Inhalation of Fine Particulate Air Pollution and Ozone Causes Acute Arterial Vasoconstriction in Healthy Adults; *Circulation* **2002**, *105*, 1534-1536.
15. Naeher, L.P.; Brauer, M.; Lipsett, M.; Woodsmoke Health Effects; *Inhal. Toxicol.* **2007**, *19*, 67-106.
16. Grahame, T.J.; Schlesinger, R.B. Health Effects of Airborne Particulate Matter; Do We Know Enough to Consider Regulating Specific Particle Types or Sources?; *Inhal. Toxicol.* **2007**, *19*, 457-481.
17. Chen, L.C.; Nadziejko, C. Effects of Subchronic Exposures to Concentrated Ambient Particles (CAPs) in Mice: V. CAPs Exacerbate Aortic Plaque Development in Hyperlipidemic Mice; *Inhal. Toxicol.* **2005**, *17*, 217-224.
18. Wellenius, G.A.; Coull, B.A.; Godleski, J.J.; Koutrakis, P.; Okabe, K.; Savage, S.T.; Lawrence, J.E.; Murthy, G.G.K.; Verrier, R.L. Inhalation of Concentrated Ambient Air Particles Exacerbates Myocardial Ischemia in Conscious Dogs; *Environ. Health Perspect.* **2003**, *111*, 402-408.

19. Sun, Q.H.; Wang, A.X.; Jin, X.M.; Natanzon, A.; Duquaine, D.; Brook, R.D.; Aguinaldo, J.G.S.; Fayad, Z.A.; Fuster, V.; Lippmann, M.; Chen, L.C.; Rajagopalan, S. Long-Term Air Pollution Exposure and Acceleration of Atherosclerosis and Vascular Inflammation in an Animal Model; *J. Am. Med. Assoc.* **2005**, *294*, 3003-3010.
20. Lundgren, L.; Skare, L.; Liden, C.; Tornling, G. Large Organic Aerosols in a Dynamic and Continuous Whole-Body Exposure Chamber Tested on Humans and on a Heated Mannequin; *Ann. Occup. Hyg.* **2006**, *50*, 705-715.
21. Sostrand, P.; Kongerud, J.; Eduard, W.; Nilsen, T.; Skogland, M.; Boe, J. A Test Chamber for Experimental Hydrogen Fluoride Exposure in Humans; *Am. Ind. Hyg. Assoc. J.* **1997**, *58*, 521-525.
22. O'Shaughnessy, P.T.; Mehaffy, J.; Watt, J.; Sigurdarson, S.; Kline, J.N. Characterization of a Hooded Human Exposure Apparatus for Inhalation of Gases and Aerosols; *J. Occup. Environ. Hyg.* **2004**, *1*, 161-166.
23. Petrovic, S.; Urch, B.; Brook, J.; Datema, J.; Purdham, J.; Liu, L.; Lukic, Z.; Zimmerman, B.; Tofler, G.; Downar, E.; Corey, P.; Tarlo, S.; Broder, I.; Dales, R.; Silverman, F. Cardiorespiratory Effects of Concentrated Ambient $PM_{2.5}$: a Pilot Study Using Controlled Human Exposures; *Inhal. Toxicol.* **2000**, *12*, 173-188.
24. Sawant, A.A.; Crocker, D.R., III; Miller, J.W.; Taliaferro, T.; Diaz-Sanchez, D.; Linn, W.S.; Clark, K.W., Gond, H., Jr. Generation and Characterization of Diesel Exhaust in a Facility for Controlled Human Exposures; *J. Air & Waste Manage. Assoc.* **2008**, *58*, 829-837; doi: 10.3155/1047-3289.58.6.829.
25. Zhi, Y.; Fund, D.C.; Kennedy, N.; Hinds, W.C.; Eiguren-Fernandaz, A. Measurements of Ultrafine Particles and Other Vehicular Pollutants inside a Mobile Exposure System on Los Angeles Freeways; *J. Air & Waste Manage. Assoc.* **2008**, *58*, 424-434; doi: 10.3155/1047-3289.58.3.424.
26. Eatough, D.J.; Benner, C.L.; Bayona, J.M.; Lamb, J.D.; Lee, M.L.; Lewis, E.A.; Hansen, L.D. Chemical Composition in Environmental Tobacco Smoke. 1. Gas-Phase Acids and Bases; *Environ. Sci. Technol.* **1989**, *23*, 679-687.
27. Pope, C.A.; Hansen, J.C.; Kuprov, R.; Sanders, M.D.; Anderson, M.N.; Eatough, D. Vascular Function and Short-Term Exposure to Fine Particulate Air Pollution; *J. Air & Waste Manage. Assoc.* **2011**, *61*, 858-863; doi: 10.3155/1047-3289.61.8.858.
28. Hughes, M.D.; Xu, Y.J.; Jenkins, P.; McMorn, P.; Landon, P.; Enache, D.I.; Carley, A.F.; Attard, G.A.; Hutchings, G. J.; King, F.; Stitt, E.H.; Johnston, P.; Griffin, K.; Kiely, C.J. Tunable Gold Catalysts for Selective Hydrocarbon Oxidation under Mild Conditions; *Nature* **2005**, *437*, 1132-1135.
29. Jiang, Z.; Luo, Z.; Zhou, H. A Simple Measurement Method of Temperature and Emissivity of Coal-Fired Flames from Visible Radiation Image and Its Application in a CFB Boiler Furnace; *Fuel* **2009**, *88*, 980-987.
30. Watson J.G.; Chow, J.C. Receptor Models for Air Quality Management; *Environ. Manage.* **2004**, *9*, 27-36.
31. Watson, J.G.; Chen, L.-W. A.; Chow, J.C.; Doraiswamy, P.; Lowenthal, D.H. Source Apportionment: Findings from the U.S. Supersites Program; *J. Air & Waste Manage. Assoc.* **2008**, *58*, 265-288; doi: 10.3155/1047-3289.58.2.265.
32. Linak, W.P.; Yoo, J.I.; Wasson, S.J.; Zhu, W.; Wendt, J.O.L.; Huggins, F.E.; Chen, Y.; Shah, N.; Huffman, G.P.; Gilmour, M. I. Ultrafine Ash Aerosols from Coal Combustion: Characterization and Health Effects; *Proc. Combust. Inst.* **2007**, *31*, 1929-1937.
33. Calkins, W.H. Investigation of Organic Sulfur-Containing Structures in Coal by Flash Pyrolysis Experiments; *Energy & Fuels* **1987**, *1*, 59-64.
34. Furuya, K.; Kato, Y.; Kikuchi, T.; Gohshi, Y. State Analysis of Sulfur in Coal and Coal Fly-Ash by Double-Crystal X-Ray-Fluorescence Spectrometry; *Mikrochim. Acta* **1983**, *2*, 263-270.
35. Grover, B.D.; Eatough, N.L.; Woolwine, W.R.; Eatough, D.J.; Cary, R.A. Modifications to the Sunset Laboratory Carbon Aerosol Monitor for the Simultaneous Measurement of $PM_{2.5}$ Nonvolatile and Semi-Volatile Carbonaceous Material; *J. Air & Waste Manage. Assoc.* **2009**, *59*, 1007-1017; doi: 10.3155/1047-3289.59.8.1007.
36. Turpin, B.J.; Lim, H. J. Species Contributions to $PM_{2.5}$ Mass Concentrations: Revisiting Common Assumptions for Estimating Organic Mass; *Aerosol Sci. Technol.* **2001**, *35*, 602-610.

About the Authors

Roman Y. Kuprov (M.Sci.) and David Buck (B.A.) are recent graduates from the Department of Chemistry and Biochemistry at Brigham Young University. C. Arden Pope III is the Mary Lou Fulton Professor at Brigham Young University. Delbert J. Eatough and Jaron C. Hansen are professors in the Department of Chemistry and Biochemistry at Brigham Young University. Please address correspondence to: Jaron C. Hansen, C100 Benson Building, Department of Chemistry and Biochemistry, Brigham Young University, Provo, UT 84602; phone: +1-801-422-4066; fax: +1-801-422-0153; e-mail: jhansen@chem.byu.edu.